Stankovich, M. T. (1980) *Anal. Biochem. 109*, 295-308.
Suzuki, H., & Ogura, Y. (1970) *J. Biochem. 67*, 277-289.
Tegoni, M., Janot, M. C., Silvestrini, M., Brunori, M., & Labeyrie, F. (1984a) *Biochem. Biophys. Res. Commun. 118*, 753-759.
Tegoni, M., Silvestrini, M. C., Labeyrie, F., & Brunori, M. (1984b) *Eur. J. Biochem. 140*, 39-45.
Tegoni, M., Janot, J. M., & Labeyrie, F. (1986) *Eur. J. Biochem. 155*, 491-503.

Tegoni, M., Janot, J. M., & Labeyrie, F. (1990) *Eur. J. Biochem. 190*, 329-342.
Visser, A. J. W. G., & Fendler, J. H. (1982) *J. Phys. Chem. 86*, 2406-2409.
Wilson, G. S. (1978) *Methods Enzymol. 54*, 396-410.
Xia, Z., & Mathews, F. S. (1990) *J. Mol. Biol. 212*, 837-863.
Xia, Z.-X., Shamala, N., Bethge, P. H., Lim, L. W., Bellamy, H. D., Xuong, N. H., Lederer, F., & Mathews, F. S. (1987) *Proc. Natl. Acad. Sci. U.S.A. 84*, 2629-2633.

Shape and Lipid-Binding Site of the Nonspecific Lipid-Transfer Protein (Sterol Carrier Protein 2): A Steady-State and Time-Resolved Fluorescence Study

Theodorus W. J. Gadella, Jr.,*,[‡] Philippe I. H. Bastiaens,[§] Antonie J. W. G. Visser,[§] and Karel W. A. Wirtz[‡]

Center for Biomembranes and Lipid Enzymology, State University of Utrecht, Padualaan 8, 3584 CH Utrecht, The Netherlands, and Department of Biochemistry, Agricultural University, Dreijenlaan 3, 6703 HA Wageningen, The Netherlands

ABSTRACT: The nonspecific lipid-transfer protein (nsL-TP) from bovine liver was studied with time-resolved and steady-state fluorescence techniques. From the decay of the intrinsic tryptophanyl fluorescence, it was estimated that the rotational correlation time of nsL-TP is 15 ns. This parameter increased only slightly upon addition of an excess of negatively charged vesicles, indicating that the basic nsL-TP is not immobilized at the membrane surface under these conditions. Binding studies using fluorescent lipid analogues revealed that nsL-TP is able to extract sn-2-(pyrenehexanoyl)phosphatidylcholine and 1-palmitoyl-2-[3-(diphenylhexatrienyl)propionyl]-sn-3-phosphocholine (DPHp-PC) from a quenched donor vesicle. The fluorescence increase resulting from this binding was poorly quenched by either acrylamide or iodide. This indicates that nsL-TP shields the bound PC molecules from the aqueous environment. Time-resolved analysis of DPH fluorescence originating from DPHp-PC bound to nsL-TP yielded a rotational correlation time of 7.4 ns. This correlation time strongly suggests that the DPH moiety of the bound molecule is immobilized and that the nsL-TP/DPHp-PC complex is not attached to the donor vesicle. In view of the longer rotational correlation time obtained for the intrinsic tryptophanyl fluorescence, we conclude that nsL-TP is highly asymmetric. The data are consistent with a model in which the shape of nsL-TP is ellipsoidal with an axis ratio of 2.8. The implications for the mode of action of nsL-TP are discussed.

The nonspecific lipid-transfer protein (nsL-TP),[1] also called sterol carrier protein 2, is one of the intracellular hydrophobic ligand binding/transfer proteins (Scallen et al., 1985; Helmkamp, 1986; Wirtz & Gadella, 1990). The protein has been purified from rat, bovine, goat, and human liver (Bloj & Zilversmit, 1977; Crain & Zilversmit, 1980; Noland et al., 1980; Poorthuis & Wirtz, 1983; Traszkos & Gaylor, 1983; Van Amerongen et al., 1987; Basu et al., 1988). The high sequence homology between rat and bovine nsL-TP (>90%) suggests an important role for the protein in cellular processes (Westerman & Wirtz, 1985; Pastuszyn et al., 1987; Morris et al., 1988). NsL-TP stimulates, in vitro, the intermembrane transfer of various lipid classes including cholesterol (Crain & Zilversmit, 1980; Chanderbhan et al., 1982; Muczynski & Stahl, 1983; North & Fleischer, 1983; Van Amerongen et al., 1989), phospholipids (Crain & Zilversmit, 1980; Nichols, 1988; Van Amerongen et al., 1989), sphingomyelin (Crain & Zilversmit, 1980), gangliosides (Bloj & Zilversmit, 1981), and neutral glycosphingolipids (Bloj & Zilversmit, 1981). As a consequence of nsL-TP-mediated transfer of cholesterol, nsL-TP was shown to stimulate microsomal conversion of

lanosterol into cholesterol (Noland et al., 1980; Traszkos & Gaylor, 1983), cholesterol esterification (Gavey et al., 1981; Poorthuis & Wirtz, 1982; Traszkos & Gaylor, 1983), bile acid formation (Seltman et al., 1985; Lidström-Olssen & Wikvall, 1986), and steroid hormone synthesis (Chanderbhan et al., 1982; Vahouny et al., 1983; Van Noort et al., 1986, 1988a,b). Although many studies have focused on the role of nsL-TP in lipid metabolism, the exact mechanism by which nsL-TP mediates the transfer of cholesterol and of phospholipids is not yet fully understood. Recently it was shown that upon equilibration with membranes containing dehydroergosterol, nsL-TP forms a water-soluble lipid/nsL-TP complex (Schroeder et al., 1990). This strongly suggests that the lip-

‡Center for Biomembranes and Lipid Enzymology, State University of Utrecht.
§Department of Biochemistry, Agricultural University.

[1] Abbreviations: nsL-TP, nonspecific lipid-transfer protein; PC, phosphatidylcholine; TNP-PE, *N*-(2,4,6-trinitrophenyl)phosphatidylethanolamine; PA, phosphatidic acid; Pyr(6)-PC, sn-2-(pyrenehexanoyl)phosphatidylcholine; DPH, 1,6-diphenyl-1,3,5-hexatriene (all trans); DPHp-PC, 1-palmitoyl-2-[3-(diphenylhexatrienyl)propionyl]-sn-3-phosphocholine; TLC, thin-layer chromatography; SDS-PAGE, sodium dodecyl sulfate–polyacrylamide gel electrophoresis; POPOP, 1,4-di-[2-(5-phenyloxazolyl)]benzene; PTF, *p*-terphenyl; IgG, immunoglobulin G; PI-TP, phosphatidylinositol-transfer protein; PC-TP, phosphatidylcholine-transfer protein; BSA, bovine serum albumin; Tris, tris(hydroxymethyl)aminomethane; EDTA, ethylenediaminetetraacetic acid; EGTA, ethylene glycol-bis-(β-aminomethyl ether)-*N,N,N′,N′*-tetraacetic acid; DMSO, dimethyl sulfoxide; DW, Durbin–Watson parameter.

id/nsL-TP complex is a key intermediate in intermembrane transfer (Nichols, 1988). In previous studies, however, attempts to isolate the nsL-TP/lipid complex were unsuccessful (Crain & Zilversmit, 1980; Van Amerongen et al., 1985). In addition, extraction of nsL-TP failed to detect any bound lipid (Crain & Zilversmit, 1980; Chanderbhan et al., 1982). These observations have led to models of transfer in which nsL-TP is part of a ternary complex between donor and acceptor membranes (Somerharju et al., 1981; Van Amerongen et al., 1985, 1989; Altamura & Landiscina, 1986; Megli et al., 1986; Billheimer & Gaylor, 1990) as well as to models in which, by binding to a membrane, nsL-TP increases the rate of dissociation of (phospho)lipid monomers from the membrane (Thompson, 1982; Nichols & Pagano, 1983).

Because nsL-TP contains a single tryptophan residue (Westerman & Wirtz, 1985) and is able to bind fluorescent lipid molecules (Nichols, 1987, 1988; Schroeder et al., 1990), it is very suitable for investigation by time-resolved and steady-state fluorescence spectroscopy. Time-resolved fluorescence spectroscopy is very powerful as it allows one to monitor the rotational dynamics of a protein molecule (Wolber et al., 1981; Visser et al., 1989). By binding a fluorescent lipid molecule to nsL-TP, the interaction between lipid and protein also becomes accessible to this technique (Berkhout et al., 1984; Van Paridon et al., 1987). Due to the high sensitivity of time-resolved fluorescence spectroscopy, it was possible to measure the interaction between nsL-TP and a fluorescent PC analogue even in the presence of vesicles containing these analogues. The results provide very strong evidence that nsL-TP is a carrier of lipids. The implications for the mode of action of nsL-TP will be discussed.

EXPERIMENTAL PROCEDURES

Materials

Egg PC and PA were obtained from Sigma (St. Louis, MO). TNP-PE was synthesized as described (Van Duijn et al., 1985). Pyrene-labeled PC species were prepared according to Somerharju et al. (1987) and kindly donated by Dr. P. J. Somerharju (University of Helsinki). DPHp-PC was obtained from Molecular Probes (Eugene, OR). The purity of the phospholipids was routinely checked by TLC. NsL-TP was purified from bovine liver (Van Amerongen et al., 1989) and stored in 5 mM sodium phosphate, 5 mM β-mercaptoethanol, 60 vol % glycerol, pH 7.4, at -20 °C. The purity of the preparation was more than 90% as estimated from SDS-PAGE. Bovine serum albumin fraction V was from Calbiochem (San Diego, CA); ovalbumin two times crystallized was from Worthington Biochemical Corporation; and cytochrome c (>99%) was from Sigma. Sephadex G-100 was purchased from Pharmacia (Uppsala, Sweden); goat anti-rabbit IgG conjugated to horseradish peroxidase was from Nordic Immunological Laboratories (Tilburg, The Netherlands); O-phenylenediamine was from Sigma; POPOP was from Eastman Kodak (Weesp, The Netherlands); PTF was from British Drug House; and microtiterplates were from Greiner (Alphen a.d. Rijn, The Netherlands). All other chemicals used were of analytical grade.

Methods

Steady-State Fluorescence Measurements. Measurements were performed on an SLM-Aminco SPF-500C fluorimeter equipped with a thermostated cuvette holder and a stirring device. The temperature was always kept at 25 °C. Pyrene-containing samples were excited at 346 nm (bandwidth 2.5 nm), and the emission was measured at 377 nm (bandwidth 10 nm). Samples containing DPHp-PC were excited at 355

nm (bandwidth 2.5 nm), and the fluorescence was recorded at 442 nm (bandwidth 10 nm). Tryptophanyl fluorescence was obtained by exciting at 280 nm (bandwidth 5 nm) and measuring an emission spectrum from 300 to 400 nm (bandwidth 10 nm). The buffers used were routinely filtered through a millipore filter (0.45 μm). All fluorescence measurements were corrected for background and inner filtering effects (if necessary).

Binding of Fluorescent Lipids. Binding of pyrene-labeled lipids to nsL-TP was performed as described for PC-TP and PI-TP (Somerharju et al., 1987; Van Paridon et al., 1988). Briefly, donor vesicles were prepared in the cuvette by injecting a mixture of 4 nmol of Pyr(6)-PC and 0.4 nmol of TNP-PE (internal quencher) dissolved in 20 μL of ethanol into buffer A (20 mM Tris-HCl, pH 7.4, 100 mM NaCl, 1 mM EGTA, and 1 mM EDTA) under continuous stirring. After a 2-min equilibration period, an aliquot of nsL-TP (100 μL, 3.4 nmol) was added (final volume 2 mL), and the increase in pyrene monomer fluorescence was measured. After completion of binding (after 2 min), the sample was subjected to quenching experiments (see below).

Binding of DPHp-PC to nsL-TP was measured similarly as described for Pyr(6)-PC, except that 6.6 nmol of DPHp-PC was injected into the cuvette and that TNP-PE was omitted from the donor vesicles. The equilibration period after addition of nsL-TP was increased to 25 min. Buffer A was argon saturated to prevent oxidation of the DPH moiety.

Quenching Experiments. In fluorescence-quenching experiments, aliquots of the quencher solutions (made in buffer A) were added directly to the sample. The fluorescence values were corrected for dilution effects. The absorbance of the samples at the excitation wavelength was always below 0.1. The KI solution used contained 0.1 mM sodium thiosulfate to inhibit formation of I_3^- (Wasylewski et al., 1988). The quenching constant K_Q was determined according to the Stern–Volmer theory (Stern & Volmer, 1919).

$$F_0/F = 1 + K_Q[Q] \tag{1}$$

where F_0 is the fluorescence observed in the absence of quencher and F is the fluorescence at a certain concentration of quencher [Q].

Gel Filtration. Prior to gel filtration, nsL-TP (1 mL, 34 nmol) was desalted on a Sephadex G15 column (5 × 1.5 cm) in 20 mM Tris-HCl, pH 7.4, 50 mM NaCl, and 0.02% (w/v) NaN₃ with and without β-mercaptoethanol (0.3% v/v). Then nsL-TP (1 mL, 20 nmol) was mixed with cytochrome c (2 mg), BSA (3 mg), and ovalbumin (3 mg) and applied onto a Sephadex G-100 column (98 × 1.0 cm) that was equilibrated with the same buffer. Fractions of 1.04 mL were collected at a flow rate of 4.17 mL/h. The conditions were chosen according to Fisher (1969). Fractions were assayed for nsL-TP by measuring transfer of Pyr(6)-PC and by enzyme immunoassay (see below).

Phospholipid-Transfer Assay. Transfer of Pyr(6)-PC from quenched donor to unlabeled acceptor vesicles was determined as described by Somerharju et al. (1987). The assay is based on the increase of pyrene monomer fluorescence upon transfer of Pyr(6)-PC from donor membranes containing quencher molecules (TNP-PE) to unquenched acceptor vesicles. Donor vesicles were prepared in the cuvette by injecting 1 nmol of Pyr(6)-PC and 0.1 nmol TNP-PE dissolved in 10 μL of ethanol into buffer A (see above) with continuous stirring. After 1 min, 20 nmol of sonicated acceptor vesicles (PC/PA, 95:5 molar ratio) were added, and the passive transfer was recorded. Subsequently, nsL-TP activity was assayed by pipetting an aliquot of 25 μL into the cuvette (final volume 2

mL). The protein-mediated transfer was corrected for the passive transfer.

Enzyme Immunoassay. Levels of nsL-TP were also determined by immunoassay as described by Teerlink et al. (1984). Briefly, nsL-TP was adsorbed to a polyvinyl microtiterplate in the presence of an excess of BSA. Then an affinity-purified polyclonal antibody was added followed by a second antibody coupled to horseradish peroxidase. NsL-TP was quantitated by the peroxidase reaction, which was initiated by addition of *o*-phenylenediamine and hydrogen peroxide. After addition of 2 M H_2SO_4, the absorption at 492 nm was measured by use of an Easy Reader EAR 400 (SLT Labinstruments, Austria).

Other Determinations. The concentration of nonlabeled phospholipids was determined by phosphorous assay (Rouser et al., 1970). The concentration of pyrene or DPH-labeled phospholipids was determined by measuring the absorbance in ethanol with extinction coefficients of $\epsilon_{342} = 42\,000$ and $\epsilon_{355} = 60\,500$ M^{-1} cm^{-1}, respectively (Somerharju et al., 1987; Lentz, 1989). The concentration of the nsL-TP stock solution was estimated by measuring the absorbance at 280 nm with an extinction coefficient of 6000 M^{-1} cm^{-1}.

Time-Resolved Fluorescence Measurements. Measurements were performed with a frequency-doubled output dye laser pumped by a mode-locked argon-ion laser as source of excitation and with time-correlated single-photon counting as a detection method. Details of the experimental setup are described by Van Hoek et al. (1987). Buffer A was used unless stated otherwise. Samples containing only nsL-TP were excited at 300 nm, whereas samples containing DPHp-PC were excited at 340 nm. Tryptophanyl fluorescence emission was passed through a Schott 338.9-nm line interference filter or through a Schott 348.8-nm interference filter together with a Schott WG 335-nm cut-off filter (Schott, Mainz, Germany). The DPH fluorescence emission was passed through a Schott KV 399-nm cut-off and a Schott 441.7-nm interference filter. Fluorescence and anisotropy decays were obtained by measuring a repeated cycle (10 s) of the parallel ($I_\parallel$) and perpendicular ($I_\perp$) fluorescence intensity components. It was found that 10–20 cycles were sufficient to give a good signal-to-noise ratio. Samples were corrected for background fluorescence (substraction of the signal of a sample lacking the fluorophore).

Data Analysis. Fluorescence and anisotropy decay curves were analyzed by an iterative nonlinear least-squares reconvolution approach, as described by Vos et al. (1987).

First the total fluorescence was calculated by combining the two intensity components $I_\parallel(t)$ and $I_\perp(t)$, which were corrected for background:

$$I_o(t) = I_\parallel(t) + 2I_\perp(t) \tag{2}$$

where $I_o(t)$ is the total observed fluorescence, which was fitted to a sum of exponentials

$$I_c(t) = \sum_i \alpha_i e^{-t/\tau_i} \tag{3}$$

in which the α_i's are the pre-exponential factors belonging to the lifetime component τ_i. $I_c(t)$ is the calculated fluorescence based on the exponential expression. The optimization was based on a minimization of the square of the difference between $I_c(t)$ and $I_o(t)$. To correct for the instrumental response, a reference reconvolution method was used, applying compounds such as POPOP or PTF with a single-exponential fluorescence decay with a lifetime of 1.35 and 1.06 ns in ethanol, respectively (Zuker et al., 1985). The observed anisotropy decay $r_o(t)$ is given by

$$r_o(t) = [I_\parallel(t) - I_\perp(t)]/I_o(t) \tag{4}$$

The anisotropy was fitted to a sum of exponentials

$$r_c(t) = \sum_j \beta_j e^{-t/\phi_j} \tag{5}$$

where $r_c(t)$ is the calculated anisotropy decay and the β_j's are the initial anisotropy components belonging to the rotational correlation times ϕ_j's. The optimization was performed by a global fit of $I_\parallel(t)$ and $I_\perp(t)$ according to

$$I_\parallel(t) = I_c(t)[1 + 2r_c(t)]/3 \tag{6}$$

$$I_\perp(t) = I_c(t)[1 - r_c(t)]/3 \tag{7}$$

Note that in this second fit the result of the total fluorescence fit $I_c(t)$ is used. Details of the procedure and the advantage over other methods have been summarized by Vos et al. (1987). The rotational correlation times are directly related to the molecular volume of the rotating object. For a spherical particle, the Stokes Einstein equation was derived:

$$\phi_S = \eta V/kT \tag{8}$$

where ϕ_S is the rotational correlation time of the sphere and η, V, k, T represent the viscosity of the medium, the volume of the particle, the Boltzmann constant, and the absolute temperature, respectively.

Associated Fit Procedure. In case of two independent populations of fluorophores (populations A and B), the total observed fluorescence as a function of time is a sum of the two populations. For both populations, the fluorescence decay and the corresponding anisotropy decay is described by a sum of exponentials (see eqs 3 and 5). The combined anisotropy of the two populations is given by

$$r_c(t) = [r_c^A(t)I_c^A(t) + r_c^B(t)I_c^B(t)]/[I_c^A(t) + I_c^B(t)] \tag{9}$$

in which $r_c^A(t)$, $r_c^B(t)$, $I_c^A(t)$, and $I_c^B(t)$ are the calculated anisotropy decays of population A and B and the calculated fluorescence decays of populations A and B, respectively. Note that this expression is different from $r_c^A(t) + r_c^B(t)$. Equation 9 can be expressed as

$$r_c(t) = \frac{\{\sum_i\sum_j \alpha_i\beta_j e^{-(1/\tau_i + 1/\phi_j)t}\} + \{\sum_k\sum_l \alpha_k\beta_l e^{-(1/\tau_k + 1/\phi_l)t}\}}{\{\sum_i \alpha_i e^{-t/\tau_i}\} + \{\sum_k \alpha_k e^{-t/\tau_k}\}} \tag{10}$$

The summations over i and j correspond to population A, whereas the summations over k and l correspond to population B. The associative fit procedure eliminates a number of cross terms between populations A and B (τ_i's are not coupled to ϕ_j's), and therefore it gives a more accurate description of the fluorescence decay process for two independent populations than a nonassociative fit procedure. For details of the description of the associated fit procedure, we refer to Dale et al. (1977) and to Ludescher et al. (1987).

RESULTS

Tryptophanyl Fluorescence. nsL-TP contains a single tryptophan residue and no tyrosine residues (Westerman & Wirtz, 1985). This makes it very suitable for intrinsic tryptophan fluorescence measurements. Upon excitation (λ_{ex} = 280–300 nm), a broad emission spectrum is observed ranging from 300 to over 400 nm, with a maximum around 330–340 nm [see also Schroeder et al. (1990)]. To assess the localization of the tryptophan residue, the tryptophan fluorescence of nsL-TP was quenched by addition of acrylamide or iodide. Quenching constants of 2.03 ± 0.03 M^{-1} and 5.24 ± 0.05 M^{-1} were obtained for iodide and acrylamide, respectively (see Table I). Control experiments with L-tryptophan in water yielded much larger quenching constants, suggesting that the tryptophan residue in nsL-TP is not exposed to the medium.

Table I: Quenching Constants of Several Fluorophores by Acrylamide and Iodide (M^{-1})

sample[a]	quencher	
	iodide	acrylamide
nsL-TP (Trp)	2.03 ± 0.03	5.24 ± 0.05
tryptophan	14.7 ± 0.1	31.2 ± 0.2
DPHp-PC	5.78 ± 0.06[b]	1.20 ± 0.01[b]
DPHp-PC in nsL-TP	0.6 ± 0.6	1.0 ± 0.8
Pyr(6)-PC	173 ± 3[b]	0.0 ± 0.01[b]
	19.5 ± 0.5[c]	0.44 ± 0.05[c]
Pyr(6)-fatty acid	52.5 ± 0.8	383 ± 58
Pyr(6)-PC in nsL-TP	2.3 ± 0.2	2.97 ± 0.07
Pyr(6)-PC in PC-TP	1.99 ± 0.07	0.33 ± 0.01
Pyr(6)-PC in PI-TP	0.3 ± 0.1	0.01 ± 0.04

[a] The solvent used was buffer A, unless stated otherwise. For experimental details see the text. [b] The solvent was DMSO. [c] In the presence of Triton X-100.

Time-Resolved nsL-TP Fluorescence. By analyzing the time-resolved fluorescence and anisotropy decay of nsL-TP, it is possible to establish whether the tryptophan residue of nsL-TP is immobilized. If so, the rotational dynamics of the protein can be determined. A typical fluorescence decay of nsL-TP in solution is shown in Figure 1A. It is evident that the decay is very complex (note the logarithmic scale of the plot). Interestingly, also for other single-tryptophan proteins, complex decays have been obtained (Beechem & Brand, 1985; Alcala et al., 1987). Analysis of the decay yielded four lifetimes for an optimal fit (see the legend to Figure 1). The mean lifetime ($\langle \tau \rangle$) was 1.82 ns at 20 °C. The four lifetimes ranging from 0.3 to about 9 ns may represent a lifetime distribution of the tryptophan fluorescence (Alcala et al., 1987). For the mathematical expression of the fluorescence decay (with fixed lifetime components), this poses no problem as one can see from the fitting parameter χ^2 of about 1.0 and the Durbin–Watson parameter (Vos et al., 1987) of about 2.0. The anisotropy decay of nsL-TP in solution was clearly single exponential (Figure 1B). Analysis of the decay yielded a rotational correlation time of 15 ns, and again the fit criteria were excellent ($\chi^2 = 1.1$, DW = 1.9). This rotational correlation time demonstrates that the tryptophan residue is immobile within the fluorescence timescale. On the other hand, a rotational correlation time of 15 ns is too large for a protein with a molecular weight of 14 kDa. To determine the molecular volume of nsL-TP, time-resolved measurements were performed at 4, 10, 20, 30, and 40 °C. The results of the experiments are shown in Table II. The average lifetime $\langle \tau \rangle$ decreases from about 2.3 ns to about 1.4 ns upon increasing the temperature from 4 to 40 °C. Also the rotational correlation time decreases with temperature from about 24 ns at 4 °C to less than 10 ns at 40 °C. Correlation times were also measured at 4 and 40 °C by using samples with 6- and 60-fold lower nsL-TP concentrations. As can be inferred from Table II, no significant changes in fluorescence and anisotropy parameters are observed upon dilution. By plotting ϕ versus η/T (eq 8), including the points corresponding to the 6- and 60-fold diluted samples, a straight line was observed for nsL-TP (Figure 2). This strongly suggests that the molecular volume remains constant with temperature between 4 and 40 °C and within a wide nsL-TP concentration range (0.17–10 μM). If a spherical shape is assumed for nsL-TP, then the slope of the line predicts a molecular volume of 35.4 ± 2.6 L/mol (eq 8). This indicates either that nsL-TP is a dimer or that the assumption of a spherical shape is wrong.

Gel Filtration. The possibility of a nsL-TP dimer was tested by molecular sieve chromatography on Sephadex G-100. Three standard proteins (BSA, ovalbumin, and cytochrome
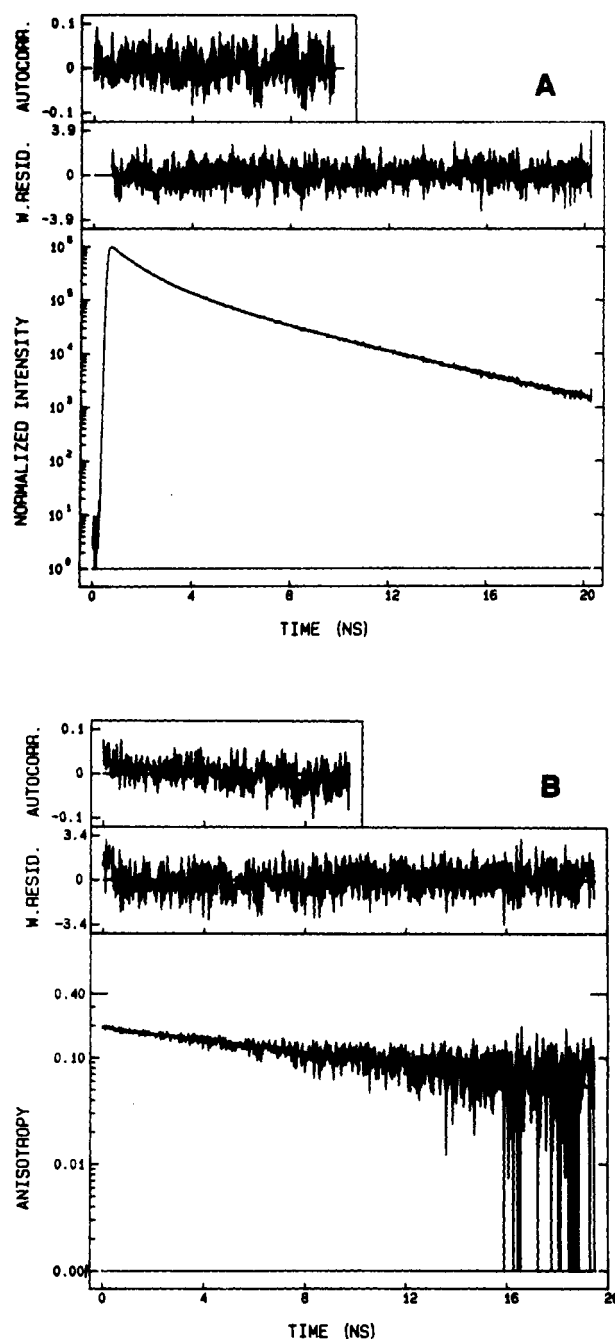

FIGURE 1: Fluorescence decay (A) and anisotropy decay (B) of nsL-TP (10 μM) in buffer at 20 °C. In panel A, both the experimental (noisy) and the calculated fluorescence decay of nsL-TP are shown (1024 channels, time equivalence 0.020 ns/channel). Background correction was performed with blank buffer. The quality of the data analysis is given by the weighted residuals and the autocorrelation of the residuals, depicted at the top of panel A. The fluorescence decay parameters for this particular fit revealed four lifetimes with $\alpha_1 = 0.29 \pm 0.01$, $\alpha_2 = 0.47 \pm 0.01$, $\alpha_3 = 0.22 \pm 0.02$, and $\alpha_4 = 0.02 \pm 0.003$ and $\tau_1 = 0.36 \pm 0.02$ ns, $\tau_2 = 1.28 \pm 0.05$ ns, $\tau_3 = 4.4 \pm 0.4$ ns, and $\tau_4 = 8.9 \pm 5.1$ ns. The statistical parameters were $\chi^2 = 1.1$ and a Durbin–Watson parameter of 2.06, and the number of zero passages in the autocorrelation function was 243 for 986 channels of analysis. In panel B, the anisotropy decay of nsL-TP is shown. The experimental anisotropy is indicated by the noisy curve, while the smooth line corresponds to the calculated anisotropy decay. The analysis was performed over the whole decay pattern of $I_{\parallel}$ and $I_{\perp}$ and revealed a single-exponential decay with initial anisotropy $\beta = 0.193 \pm 0.001$ and a rotational correlation time $\phi = 15.0 \pm 0.2$ ns. The weighted residuals and the autocorrelation between them are shown on top of the curves. Statistical parameters were $\chi^2 = 1.11$ and a Durbin–Watson parameter of 1.91. The number of zero passages in the parallel and perpendicular autocorrelation functions were 233 and 235, respectively, for 983 channels of analysis.

Table II: Fluorescence and Anisotropy Decay Parameters of nsL-TP at Various Temperatures and nsL-TP Concentrations[a]

[nsL-TP] (μM)[b]	T (°C)	$\langle\tau\rangle$ (ns)[c]	β (± 0.002)	ϕ (ns)	χ^{2d}	DW[d]
0.17	4	2.76	0.210	27.4 ± 1.4	1.04	1.96
1.7	4	2.25	0.201	24.3 ± 0.4	1.06	1.96
10	4	2.27	0.201	21.5 ± 0.5	1.01	1.95
10	10	2.07	0.195	18.1 ± 0.3	1.01	1.88
10	20	1.83	0.193	15.0 ± 0.2	1.11	1.91
10	30	1.62	0.187	11.5 ± 0.2	1.05	1.91
0.17	40	1.62	0.187	7.9 ± 0.4	1.00	1.94
1.7	40	1.38	0.178	9.8 ± 0.2	1.05	1.94
10	40	1.42	0.180	9.0 ± 0.1	1.08	1.87

[a] The emission was passed through a Schott 348.8-nm interference filter and a WG 335 cut-off filter. The data were obtained and analyzed as described under Experimental Procedures. The fluorescence decay analysis (parameters not shown) yielded χ^2 = 1.0-1.1 and Durbin-Watson parameters of 1.8-2.0 for all fits. [b] The samples with a 10 μM nsL-TP concentration were desalted and did not contain glycerol or β-mercaptoethanol. The 1.7 μM samples contained glycerol (3% v/v) and β-mercaptoethanol (0.0015% v/v). For the 0.17 μM samples, these percentages were 10-fold lower. [c] Mean lifetime as analyzed from the decay parameters (not shown): $\langle\tau\rangle = \sum_i\alpha_i\tau_i$. [d] Statistical parameters for the anisotropy decay fit.
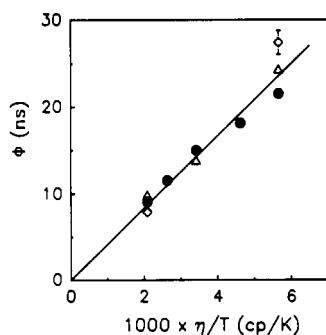

FIGURE 2: Stokes-Einstein relationship for nsL-TP-tryptophan fluorescence at different temperatures and nsL-TP concentrations. The rotational correlation times (ϕ) of nsL-TP (Table III) are plotted against the viscosity of the medium (η) divided by the absolute temperature (T). The concentrations of nsL-TP was 10 μM (●), 1.7 μM (▲), or 0.17 μM (◇).

FIGURE 3: Gel filtration of nsL-TP on Sephadex-G100. NsL-TP was desalted and applied on Sephadex-G100 together with BSA, ovalbumin, and cytochrome c. Panel A depicts the standard protein elution pattern as indicated by the absorbance at 280 nm. The three peaks correspond to BSA (fraction 40), ovalbumin (fraction 44), and cytochrome c (fraction 60), respectively. Panel B represents the nsL-TP elution profile as assayed by immunoassay (EIA) and by fluorescent transfer assay. For experimental details see Methods.

c) were included in the gel-filtration experiment (Figure 3A). In the absence of β-mercaptoethanol, nsL-TP coeluted with cytochrome c, as can be seen from the transfer activity and nsL-TP immunoresponse profiles (Figure 3B). From this it is concluded that nsL-TP behaves as a monomeric protein (M_w 13 kDa). The possibility that a large fraction of the protein was in a dimeric state and inactive in transfer was ruled out by the fact that immunological screening of the column failed to identify another peak. In the presence of β-mercaptoethanol (0.3% v/v) virtually identical results were obtained (data not shown). In agreement with this, the fluorescence decay parameters and the rotational correlation time of nsL-TP are not altered upon addition of β-mercaptoethanol (see Table III).

Interaction with Membranes. Since nsL-TP is a positively charged protein at physiological pH (Westerman & Wirtz, 1985), one may suspect that nsL-TP interacts with negatively charged membranes. To test this hypothesis, time-resolved tryptophan fluorescence measurements were performed. In the presence of an excess of PC vesicles containing 10 or 20 mol % PA, the average fluorescence lifetime $\langle\tau\rangle$ remained 1.82 ns (Table III). Since $\langle\tau\rangle$ is directly proportional to the quantum yield of the tryptophan fluorescence (Kulinski et al., 1987), its invariance predicts an unaltered steady-state fluorescence in the presence of negatively charged vesicles. This was confirmed by measuring steady-state emission spectra of nsL-TP (data not shown).

In the case of the vesicles containing 20 mol % PA, the rotational correlation time of nsL-TP was increased to 17.4 ns (Table III). From this observation it can be concluded that nsL-TP interacts weakly with negatively charged membranes. For comparison, an immobilization of nsL-TP at the surface of the vesicle would have resulted in a rotational correlation
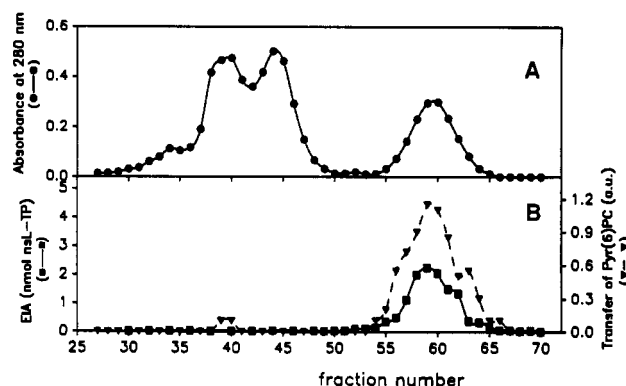
Table III: Effect of β-Mercaptoethanol and Negatively Charged Vesicles on the Fluorescence and Anisotropy Parameters of nsL-TP[a]

addition	$\langle\tau\rangle$ (ns)[b]	β (± 0.001)	ϕ (ns)	χ^{2c}	DW[c]
none	1.81	0.187	13.8 ± 0.2	1.03	1.81
β-mercaptoethanol (0.3% v/v)	1.90	0.182	15.6 ± 0.2	1.03	1.91
PC/PA (10 mol %) vesicles (100 μM)	1.81	0.192	15.0 ± 0.3	0.97	1.90
PC/PA (20 mol %) vesicles (100 μM)	1.82	0.189	17.4 ± 0.3	1.11	1.94

[a] The measurements were performed at 20 °C. The nsL-TP concentration was 1.7 μM. The samples contained glycerol (0.3% v/v) and β-mercaptoethanol (0.0015% v/v) (except for the second sample). The emission was passed through a Schott 338.9-nm line interference filter. For further experimental details and analysis procedure, see Methods. The fluorescence decay analysis yielded χ^2 = 0.96-1.0 and Durbin-Watson parameters of 1.9-2.0 for all fits (data not shown). [b] Mean lifetime as analyzed from the decay parameters (not shown): $\langle\tau\rangle = \sum_i\alpha_i\tau_i$. [c] Statistical parameters for the anisotropy decay fit.

time in the microsecond range (see below).

Phospholipid Binding. Recent studies have shown that nsL-TP is able to extract lipid molecules from a vesicle membrane (Nichols, 1987, 1988; Schroeder et al., 1990). We have confirmed this property by using vesicles consisting of Pyr(6)-PC and TNP-PE (as an internal fluorescence quencher, see Methods). Addition of nsL-TP to these vesicles resulted in a large increase in pyrene monomer fluorescence due to the movement of the Pyr(6)-PC molecule from the quenched vesicle to nsL-TP in which the fluorescence is not quenched.

Table IV: Fluorescence Decay Parameters of DPHp-PC[a]

condition	α_1	α_2	α_3	α_4	τ_1 (ns)	τ_2 (ns)	τ_3 (ns)	τ_4 (ns)	$\langle\tau\rangle$ (ns)	χ^2	DW
DPHp-PC (pop. A)	0.967	0.033			0.144	6.08			0.34	1.06	1.76
DPHp-PC+nsL-TP (pop. A + B)	0.516	0.018	0.41	0.061	0.144	6.08	4.71	7.8	5.12[b]	0.98	1.89

[a] For experimental details see Methods. The standard deviation was in the last digit of the presented data. [b] $\langle\tau\rangle$ of population B ($\alpha_3\tau_3 + \alpha_4\tau_4$).
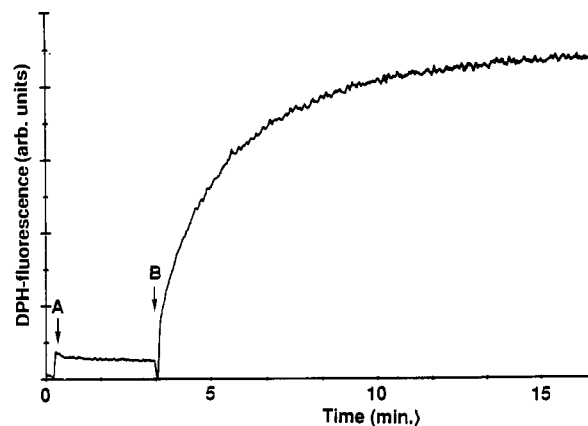

FIGURE 4: Binding of DPHp-PC to nsL-TP. Arrow A indicates the injection of 6.6 nmol of DPHp-PC dissolved in 20 μL of ethanol into 1880 μL of the buffer A. Arrow B corresponds to the addition of 100 μL of nsL-TP (3.4 nmol). Excitation and emission wavelengths were set at 355 nm (bandwidth 2.5 nm) and 432 nm (bandwidth 10 nm), respectively. The sudden drop in the signal at each addition is due to closing of the emission shutter.

Under these conditions of binding, it could be estimated that about 8% of the nsL-TP molecules contained a Pyr(6)-PC molecule. This limited binding reflects the equilibrium of the Pyr(6)-PC molecule between the vesicle and the low-affinity binding site on nsL-TP (Gadella and Wirtz, manuscript in preparation). To investigate the interaction of the fluorophore with the lipid-binding site, quenching experiments were carried out with iodide and acrylamide. Neither of the two compounds were able to efficiently quench the pyrene monomer fluorescence (K_Q = 2.3 and 2.97 M^{-1}, respectively), suggesting that the fluorophore was shielded from the medium. Similar experiments with PC-TP or PI-TP, which are known to bind one phospholipid molecule inside a lipid-binding site (Berkhout et al., 1984; Van Paridon et al., 1987), also yielded very low quenching constants for both quenchers (see Table I). For comparison, iodide and acrylamide very efficiently quenched Pyr(6)-fatty acid in water, with quenching constants of 53 and 383 M^{-1}, respectively. Iodide was also a very efficient quencher of Pyr(6)-PC mixed with Triton X-100 or dissolved in DMSO (Table I).

Binding experiments were also carried out with a diphenylhexatrienyl-labeled analogue of PC, DPHp-PC. Vesicles prepared of this PC are poorly fluorescent due to self quenching. Upon addition of nsL-TP, a striking increase in DPH-fluorescence is observed showing that DPHp-PC can be bound by nsL-TP (Figure 4). Calibration of the fluorescence signal revealed that 2% of the nsL-TP molecules contained a DPHp-PC molecule. Attempts to isolate the nsL-TP/DPHp-PC complex have failed (see Discussion) since removal of the vesicles led to a dissociation of this complex. As was observed with Pyr(6)-PC, acrylamide and iodide were inefficient quenchers of DPH-PC bound to nsL-TP ($K_Q \approx 1$ M^{-1}, see Table I). Control experiments, however, showed that the fluorescence of freely accessible DPHp-PC in DMSO cannot be very efficiently quenched by these compounds either.

Time-Resolved DPHp-PC Fluorescence. Time-resolved fluorescence measurements can provide information about the rotational freedom of a lipid molecule bound to a protein

Table V: Anisotropy Decay Parameters of DPHp-PC

condition	β_A	β_B	ϕ_A (μs)	ϕ_B (ns)	χ^2	DW
DPHp-PC (pop. A)	0.28 ● 0.00		>10		1.17	1.86
DPHp-PC + nsL-TP (pop. A + B)	0.28 $-^a$	0.336 ● 0.002	15 $-^a$	7.43 ± 0.05	1.02	1.98

[a] No standard deviation due to fixation.

(Berkhout et al., 1984; Van Paridon et al., 1987). Pyrene has a very long fluorescence lifetime (>100 ns), a low initial anisotropy, and complex photophysics. Therefore, time-resolved anisotropy experiments with Pyr(6)-PC bound to nsL-TP, which we have carried out, were very difficult to interprete (data not shown). The results obtained with DPHp-PC binding, however, were unequivocal. Due to self-quenching, the fluorescence of DPHp-PC in vesicles is very low (Figure 4). In agreement with this observation, the decay of DPHp-PC fluorescence is very fast (Figure 5A). Analysis yielded two lifetimes: a major very short component of 0.144 ns and a minor longer component of 6.1 ns (Table IV). The average lifetime $\langle\tau_A\rangle$ was 0.34 ns. Upon addition of nsL-TP to the vesicles, the fluorescence decay of DPHp-PC is much slower due to the fact that DPHp-PC incorporated into nsL-TP is not quenched (Figures 4 and 5B). In this situation there are two populations of DPHp-PC molecules: one population resides in the vesicle with a short lifetime (population A), and another population resides inside the protein and has a longer lifetime (population B). In order to analyze this decay, an associated fit method was employed in which the lifetimes for DPHp-PC fluorescence in the vesicles (population A) were used and fixed. An optimal fit was obtained by including two additional lifetimes of 4.7 and 7.8 ns (Table IV). These lifetimes are taken to originate from DPHp-PC bound to nsL-TP (population B). The average lifetime for population B is 5.1 ns, which is clearly longer than that found for population A (0.34 ns). From Figure 5B it can be seen that the contribution of population A to the fluorescence decay is restricted to the "spike" in the first part of the curve (0–0.5 ns).

The dynamic fluorescence behavior of DPHp-PC in vesicles was further analyzed by determining the time-resolved fluorescence anisotropy. Figure 6A shows that the anisotropy of DPHp-PC in vesicles remained nearly constant in the measured time interval. As a result the rotational correlation time is infinitely long as compared to the fluorescence lifetime (Table V). From this very long rotational correlation time, it may be concluded that the DPH moiety in the vesicle has no motional freedom. The low initial anisotropy (0.28) is very likely the result of energy transfer between neighboring DPH moieties ("homo-transfer") that relative to one another are slightly differently oriented. This very fast process ($\approx$ picosecond) was not resolved under the experimental conditions. Addition of nsL-TP to the DPHp-PC vesicles results in a decay of anisotropy that reflects the rotation of the DPHp-PC/nsL-TP complex (Figure 6B). Analysis of the anisotropy decay made use of an optimization procedure in which the infinitely long correlation time for DPHp-PC in vesicles (population A) and the corresponding initial anisotropy (0.28) were fixed and associated with the fluorescent lifetimes of 0.14 and 6.1 ns (see Table IV). The anisotropy decay of population B (the
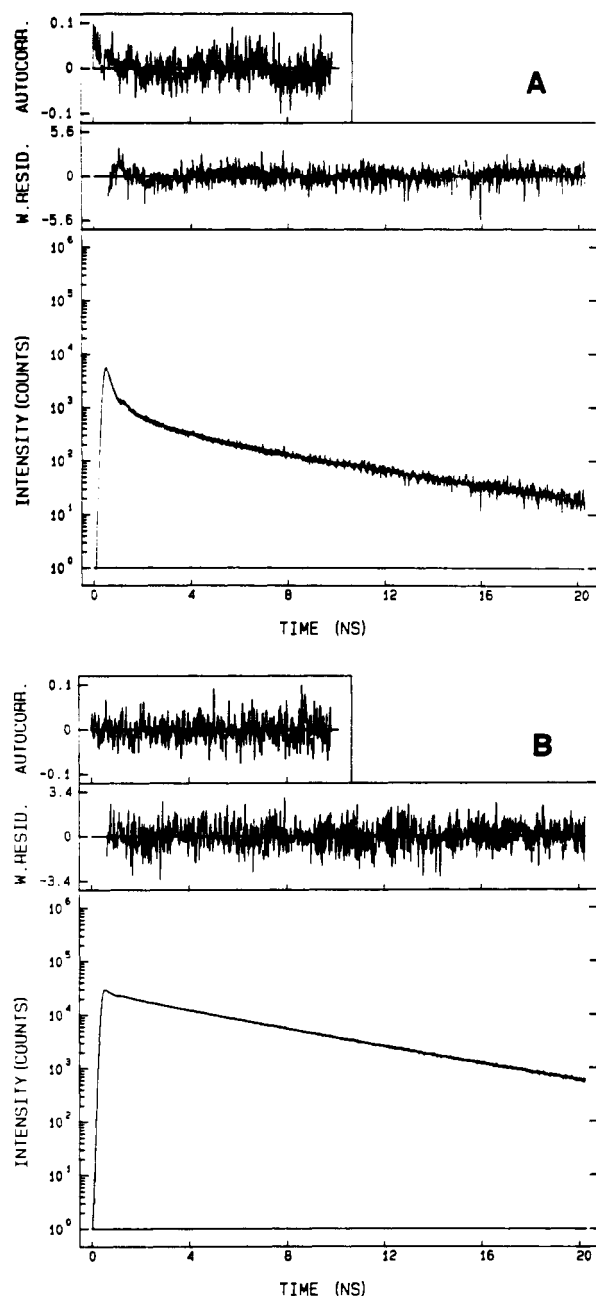
FIGURE 5: Fluorescence decay of DPHp-PC in the absence (A) and presence (B) of nsL-TP. Plot A represents 2 μM DPHp-PC vesicles, and plot B represents the situation after addition of 1.7 μM nsL-TP. For further experimental details, see Methods. The experimental and calculated fluorescence decay is shown in both plots (1024 channels, 0.020 ns each). Analysis of plot A yielded two lifetime components (see Table IV). These lifetimes were used in the fit for plot B, and two additional lifetimes were optimized (see Table IV). For both plots, the weighted residuals and their autocorrelation are shown. For details of the analysis procedure see Methods.

FIGURE 6: Anisotropy decay of DPHp-PC in the absence (A) and in the presence (B) of nsL-TP. The experimental conditions were identical with those of Figure 5. In plot A, the anisotropy decay of the DPHp-PC vesicles is shown (noisy curve) together with the calculated anisotropy decay obtained by using the parameters listed in Table V. In plot B, the anisotropy decay of the DPHp-PC vesicles in the presence of nsL-TP is shown. Analysis was performed by using an associative fit procedure (see Results and Methods) and yielded the smooth curve. For both plots, the quality of the fits are depicted on top of the plots by the weighted residuals and the autocorrelation functions.

DPHp-PC/nsL-TP complex) was consequently coupled to the lifetimes to 4.7 and 7.8 ns. The optimization procedure (see Methods) indicated that this decay could be fitted to a single-exponential function yielding a correlation time of 7.43 $\pm$ 0.05 ns (Table V). An excellent fit was obtained ($x^2 = 0.98$ and Durbin–Watson parameter = 1.9), which is remarkable in view of the constraints used. Additional experiments with different nsL-TP concentrations gave rise to a very similar rotational correlation time (data not shown). By a close look at the anisotropy decay, both populations A and B can be discriminated (Figure 6B). In the first part of the decay (0–0.5 ns), anisotropy remains nearly constant due to the fact that most of the photons emitted originate from population A,
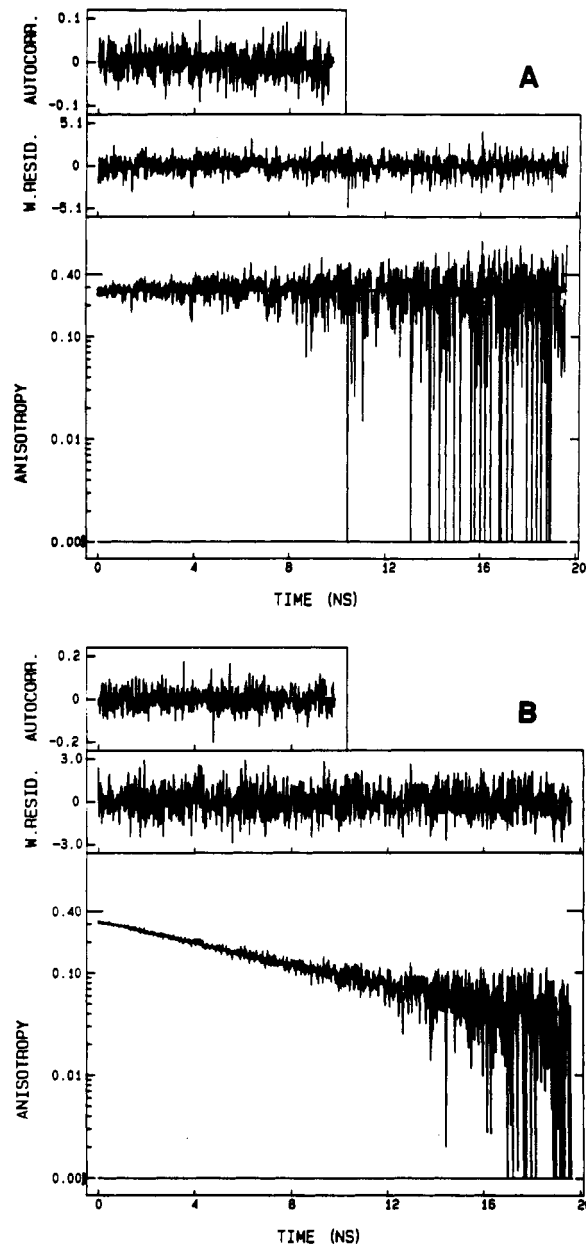
which has the very long rotational correlation time. The decay of anisotropy from 0.5 to 20 ns reflects the rotation of population B. Since this decay is described by a single rotational correlation time (7.4 ns), one may infer that DPHp-PC is completely immobilized in the binding site on nsL-TP. To reconcile this correlation time of 7.4 ns with that of 15 ns obtained from the tryptophanyl fluorescence decay, we propose that the shape of nsL-TP is ellipsoidal and that the DPHp moiety is perpendicularly oriented to the long axis of the protein (Figure 7, see Discussion).

DISCUSSION

In this study we have investigated the physical properties of nsL-TP by using fluorescence techniques. Analysis of the
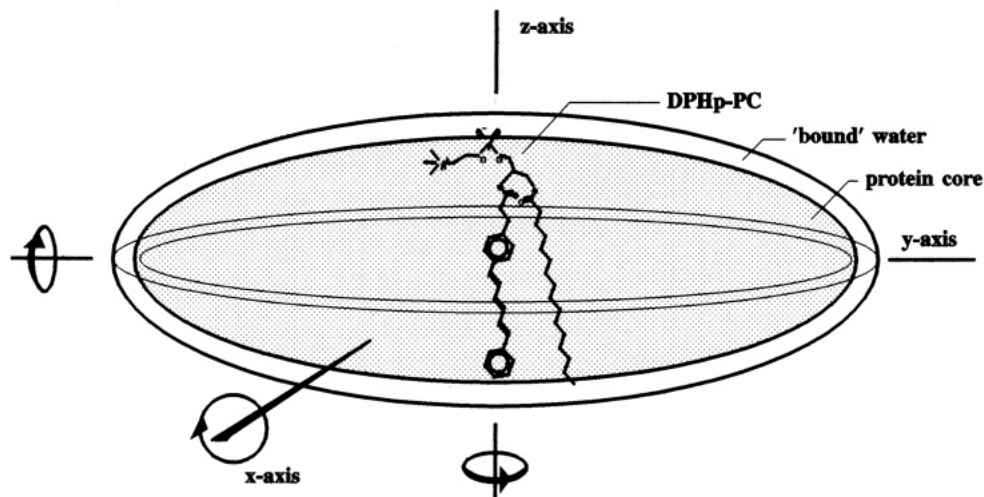
FIGURE 7: Model for nsL-TP. For an explanation, see Discussion.

time-resolved tryptophan fluorescence yielded a rotational correlation time of 15 ns (Figure 1B), whereas analysis of the DPH fluorescence of the nsL-TP/DPHp-PC complex yielded a rotational correlation time of 7.4 ns (Table V). The fact that in both instances the anisotropy decay could be described by a single-exponential function indicates that the tryptophanyl residue and the bound DPHp-PC molecule are immobilized following the rotation of nsL-TP. This being the case, the difference between the rotational correlation times strongly suggests that the molecule is nonspherical. If one postulates a prolate ellipsoid shape for nsL-TP, the rotational correlation times fit in a model in which the tryptophan and the DPH fluorescence emission dipoles are oriented parallel and perpendicular to the long symmetry axis of the molecule, respectively (see Figure 7). Consequently, the tryptophan fluorophore probes the slow rotation of nsL-TP perpendicular to this axis and the DPH fluorophore the fast rotation parallel to this axis. On the basis of these assumptions, the dimensions of nsL-TP were calculated by using the equations for the time-resolved anisotropy decay for a prolate ellipsoid molecule as derived by Perrin (1934, 1936), Tao (1969), Brandt et al. (1985), and Visser et al. (1989). This calculation for a prolate ellipsoid yielded a rotational correlation time of 15 ns for the rotation along the short axis of symmetry (*x*- or *z*-axis) and 6.6 ns for the rotation along the long symmetry axis (*y*-axis). Here it is assumed that the single rotational correlation time observed for DPHp-PC (7.4 ns) is a harmonic mean of the 15- and 6.6-ns rotational correlation times (Dale et al., 1977). From the difference between the latter correlation times, an axial ratio of 2.8 and an equivalent spherical rotational correlation time of 7 ns were calculated (Fleming, 1986; Visser et al., 1989). This is consistent with a molecular volume of 17 000 cm^3/mol (eq 8). If it is assumed that the density of anhydrous nsL-TP is 1.2 g/cm^3, the volume of the protein core (M_w 14 kDa) is 11 700 cm^3/mol, from which it is inferred that nsL-TP would contain 0.38 g of bound H_2O per gram of anhydrous protein. This degree of hydration agrees with observations made for other low molecular weight proteins (Cantor & Schimmel, 1980). It is very interesting that PC-TP is also asymmetric with an estimated axial ratio of 2.50 (Berkhout et al., 1984). An ellipsoid shape might be important for transfer proteins to interact efficiently with the membrane. Moreover, it was estimated that in PC-TP the *sn*-1 and *sn*-2 acyl chains of the bound PC molecule make an angle of 60°–90° with one another, with the *sn*-2 acyl chain perpendicular to the long symmetry axis (Berkhout et al., 1984). As for nsL-TP, our model predicts that the *sn*-2 acyl chain of the

bound DPHp-PC molecule is also perpendicular to the long symmetry axis. This follows directly from the fact that the DPH emission dipole moment is aligned along the symmetry axis of the cylindrical DPH fluorophore (Van der Meer, 1988). We do not yet know the orientation of the *sn*-1 acyl chain relative to the *sn*-2 acyl chain. The orientation of the *sn*-1 acyl chain as drawn in the model is purely speculative (Figure 7).

Previous studies provided some evidence for a nsL-TP dimer (Pastuszyn et al., 1987) in which the sulfhydryl group was believed to play a role (Wirtz & Gadella, 1990). In this study, in agreement with the findings of Crain and Zilversmit (1980) and of Poorthuis et al. (1981), we could not get any indication for the occurrence of a dimer since the rotational correlation time of nsL-TP and its behavior on molecular sieve were very similar in the absence or presence of an excess of β-mercaptoethanol (Tables II and III, Figure 3). This monomeric form also explains the constant molecular volume at different temperatures and at different concentrations (Table II, Figure 2).

In agreement with previous studies on the binding of fluorescently labeled PC and cholesterol analogues (Nichols et al., 1987, 1988; Schroeder et al., 1990), we have shown that nsL-TP is able to form a complex with PC. However in contrast to what was observed with PC-TP and PI-TP, this complex could not be isolated (data not shown). Apparently, this complex occurs only when vesicles are present. This is interpreted to indicate that lipid monomers rapidly equilibrate between a low-affinity lipid-binding site on nsL-TP and the vesicles [see also Nichols (1988)].

The localization of the fluorescent PC analogues bound to nsL-TP was further investigated by use of the collisional quenchers iodide and acrylamide. The quenching constants for DPHp-PC bound to nsL-TP were low. However, control experiments of DPHp-PC in DMSO indicated that DPH fluorescence is poorly quenched by iodide or acrylamide. Results were much more unequivocal when the quenching of the fluorescence of Pyr(6)-PC bound to nsL-TP was determined (Table I). The quenching constant (K_Q = 2.3 M^{-1} by I^-) is of the same order as observed for Pyr(6)-PC bound to PC-TP or PI-TP and two orders of magnitude lower than observed for the quenching of Pyr(6)-PC in DMSO. These experiments show that, like PC-TP and PI-TP, nsL-TP is able to shield the *sn*-2 acyl chain of the bound PC molecule from the aqueous environment.

In this study we have also investigated the interaction of nsL-TP with membranes by measuring the decay of tryptophanyl fluorescence anisotropy. Upon addition of a large excess of negatively charged vesicles, the rotational correlation

time of the protein increased only slightly to 17.4 ns (Table III). From this it is concluded that a complete immobilization of nsL-TP at the vesicle interface does not occur (Osada et al., 1984). In view of the resolution of the anisotropy decay, it cannot be excluded that a minor fraction of nsL-TP does become immobilized. From the data with the vesicles containing 20% PA, it could be estimated that the bound fraction would constitute less than 9% of the total nsL-TP. On the other hand, the slight increase in the rotational correlation time is best explained by assuming that a weak interaction of nsL-TP with membranes hinders the rotation. The demonstration that nsL-TP hardly interacts with negatively charged vesicles argues against the proposed model in which nsL-TP brings two membranes together due to strong electrostatic interactions (Somerharju et al., 1981; Van Amerongen et al., 1989; Wirtz & Gadella, Jr., 1990; Billheimer & Gaylor, 1990).

Binding of DPHp-PC and Pyr(6)-PC to nsL-TP is in agreement with a carrier model as proposed by Nichols (1987, 1988). The time-resolved fluorescence measurements of the DPHp-PC/nsL-TP complex show that this complex is not hindered in its rotation. The lack of limiting anisotropy (Figure 6B) indicates that this complex is not attached to the membrane interface. On the other hand, an interaction between nsL-TP and membranes is very likely to precede the formation of the complex. Our findings suggest that this interaction is weak as also observed by Nichols (1987). The significance of this interaction follows from the observations that introduction of negative charges in the donor vesicle greatly enhanced the transfer rate of dehydroergosterol and cholesterol by nsL-TP (Butko et al., 1990; Billheimer & Gaylor, 1990).

Concluding, we propose a mechanism of nsL-TP-mediated transfer involving a transient interaction with membranes and a subsequent dissociation of a nsL-TP/lipid complex from the interface. This must be a low-affinity complex since, upon removal of the membranes, the bound lipid leaves the protein. This explains the impossibility of isolating the lipid/protein complex (Nichols, 1987; Crain & Zilversmit, 1980) and the inability of the protein to catalyze exchange between two separated monolayers (Van Amerongen et al., 1989). The apparent paradox between the low-affinity binding site of the protein (Nichols et al., 1988; Schroeder et al., 1990) on the one hand, and the complete immobilization of the DPH moiety upon binding of DPHp-PC and the inability to quench its fluorescence by water-soluble quenchers on the other hand, is explained by the great difference in time scales of the binding process (millisecond range) and the fluorescence process (nanosecond range). In fact, the immobilization of the DPH moiety on the DPH-fluorescence timescale indicates that the lifetime of the lipid/nsL-TP complex is longer than hundreds of nanoseconds. The striking correlation between passive and nsL-TP-mediated transfer (Thompson, 1982; Van Amerongen et al., 1989), which must be incorporated in a complete model for the mode of action of nsL-TP, remains to be explained.

REFERENCES

Alcala, J. C., Gratton, E., & Prendergast, F. G. (1987) *Biophys. J. 51*, 925–936.

Altamura, N., & Landriscina, C. (1986) *Int. J. Biochem. 18*, 513–517.

Basu, J., Kundu, M., Bhuttacharya, U., Mazumder, C., & Chakrabarti, P. (1988) *Biochim. Biophys. Acta 959*, 134–142.

Beechem, J. M., & Brand, L. (1985) *Annu. Rev. Biochem. 54*, 43–71.

Berkhout, T. A., Visser, A. J. W. G., & Wirtz, K. W. A. (1984) *Biochemistry 23*, 1505–1513.

Billheimer, J. T., & Gaylor, J. L. (1990) *Biochem. Biophys. Acta 1046*, 136–143.

Bloj, B., & Zilversmit, D. B. (1977) *J. Biol. Chem. 252*, 1613–1619.

Bloj, B., & Zilversmit, D. B. (1981) *J. Biol. Chem. 256*, 5988–5991.

Brand, L., Knutson, J. R., Davenport, L., Beechem, J. M., Dale, R. E., Walbridge, D. G., & Kowalczyk, A. A. (1985) in *Spectroscopy and Dynamics of Biological Systems* (Bayley, P. B., & Dale, R. E., Eds.) pp 259–305, Academic Press, London.

Butko, P., Hapala, I., Scallen, T. J., & Schroeder, F. (1990) *Biochemistry 29*, 4070–4077.

Cantor, C. R., & Schimmel, P. R. (1980) *Biophysical Chemistry*, Part II, p 552, W. H. Freeman, San Francisco, CA.

Chanderbhan, R., Noland, B. J., Scallen, T. J., & Vahouny, G. V. (1982) *J. Biol. Chem. 257*, 8928–8934.

Crain, R. C., & Zilversmit, D. B. (1980) *Biochemistry 19*, 1433–1439.

Dale, R. E., Chen, L. A., & Brand, L. (1977) *J. Biol. Chem. 252*, 7500–7510.

Fisher, L. (1969) in *Laboratory Techniques in Biochemistry and Molecular Biology* (Work, T. S., & Work, E., Eds.) Vol. I, pp 175–390, North-Holland Publishing Company, Amsterdam.

Fleming, G. R. (1986) in *Chemical Applications of Ultrafast Spectroscopy*, pp 132–133, Oxford University Press, New York.

Gavey, K. L., Noland, B. J., & Scallen, T. J. (1981) *J. Biol. Chem. 256*, 2993–2999.

Helmkamp, G. M. (1986) *J. Bioenerg. Biomembr. 18*, 71–91.

Kulinski, T., Visser, A. J. W. G., O'Kane, D. J., & Lee, J. (1987) *Biochemistry 26*, 540–549.

Lentz, B. R. (1989) *Chem. Phys. Lipids 50*, 171–190.

Lidström-Olssen, B., & Wikvall, K. (1986) *Biochem. J. 238*, 879–884.

Ludescher, R. D., Peting, L., Hudson, S., & Hudson, B. (1987) *Biophys. Chem. 28*, 59–75.

Megli, F. M., De Lisi, A., Van Amerongen, A., Wirtz, K. W. A., & Quagliariello, E. (1986) *Biochim. Biophys. Acta 861*, 463–470.

Morris, H. R., Larsen, B. S., & Billheimer, J. T. (1988) *Biochem. Biophys. Res. Commun. 154*, 476–482.

Muczynski, K. A., & Stahl, W. L. (1983) *Biochemistry 22*, 6037–6048.

Nichols, J. W. (1987) *J. Biol. Chem. 262*, 14172–14177.

Nichols, J. W. (1988) *Biochemistry 27*, 1889–1896.

Nichols, J. W., & Pagano, R. E. (1983) *J. Biol. Chem. 258*, 5368–5371.

Noland, B. J., Arebalo, R. E., Hansbury, E., & Scallen, T. J. (1980) *J. Biol. Chem. 255*, 4282–4289.

North, P., & Fleisher, S. (1983) *Methods Enzymol. 98*, 599–613.

Gadella et al.

Osada, H., Nakanishi, M., Tsuboi, M., Kinosita, K., Jr., & Ikegami, A. (1984) *Biochim. Biophys. Acta 773*, 321–324.

Pastuszyn, A., Noland, B. J., Bazan, J. F., Fletterick, R. J., & Scallen, T. J. (1987) *J. Biol. Chem. 262*, 13219–13227.

Perrin, F. (1934) *J. Phys. Radium 5*, 497–511.

Perrin, F. (1936) *J. Phys. Radium 7*, 1–11.

Poorthuis, B. J. H. M., & Wirtz, K. W. A. (1982) *Biochim. Biophys. Acta 710*, 99–105.

Poorthuis, B. J. H. M., & Wirtz, K. W. A. (1983) *Methods Enzymol. 98*, 592–596.

Poorthuis, B. J. H. M., Glatz, J. F. C., Akeroyd, R., & Wirtz, K. W. A. (1981) *Biochim. Biophys. Acta 665*, 256–261.

Rouser, G., Fleisher, S., & Yamamoto, A. (1970) *Lipids 5*, 494–496.

Scallen, T. J., Pastuszyn, A., Noland, B. J., Chanderbhan, R., Kharoubi, A., & Vahouny, G. V. (1985) *Chem. Phys. Lipids 38*, 239–261.

Schroeder, F., Butko, P., Nemecz, G., & Scallen, T. J. (1990) *J. Biol. Chem. 265*, 151–157.

Seltman, H., Diven, W., Rizk, M., Noland, B. J., Chanderbhan, R., Scallen, T. J., Vahouny, G. V., & Sanghvi, A. (1985) *Biochem. J. 230*, 19–24.

Somerharju, P. J., Brockerhoff, H., Jackson, R. L., & Wirtz, K. W. A. (1981) *Biochim. Biophys. Acta 649*, 521–528.

Somerharju, P. J., Van Loon, D., & Wirtz, K. W. A. (1987) *Biochemistry 26*, 7193–7199.

Stern, O., & Volmer, M. (1919) *Phys. Z. 20*, 183–188.

Tao, T. (1969) *Biopolymers 8*, 609–632.

Teerlink, T., Van der Krift, T. P., Van Heusden, G. P. H., & Wirtz, K. W. A. (1984) *Biochim. Biophys. Acta 793*, 251–259.

Thompson, T. E. (1982) *J. Am. Oil Chem. Soc. 59*, 309A.

Traszkos, J. M., & Gaylor, J. L. (1983) *Biochim. Biophys. Acta 751*, 52–65.

Vahouny, G. V., Chanderbhan, R., Noland, B. J., Irwin, D., Dennis, P., Lambeth, J. D., & Scallen, T. J. (1983) *J. Biol. Chem. 258*, 11731–11737.

Van Amerongen, A., Teerlink, T., Van Heusden, G. P. H., & Wirtz, K. W. A. (1985) *Chem. Phys. Lipids 38*, 195–204.

Van Amerongen, A., Helms, J. B., Van der Krift, T. P., Schutgens, R. B. H., & Wirtz, K. W. A. (1987) *Biochim. Biophys. Acta 919*, 149–155.

Van Amerongen, A., Demel, R. A., Westerman, J., & Wirtz, K. W. A. (1989) *Biochim. Biophys. Acta 1004*, 36–43.

Van der Meer, B. W. (1988) in *Subcellular Biochemistry* (Hilderson, H. J., & Harris, J. R., Eds.) Vol. 13, pp 1–53, Plenum Press, New York.

Van Duijn, G., Dekker, J., Leunissen-Bijvelt, J., Verkley, A. J., & de Kruijff, B. (1985) *Biochemistry 24*, 7640–7650.

Van Hoek, A., Vos, K., & Visser, A. J. W. G. (1987) *IEEE J. Quantum Electron. 23*, 1812–1820.

Van Noort, M., Rommerts, F. F. G., Van Amerongen, A., & Wirtz, K. W. A. (1986) *J. Endocrinol. 109*, R13–R16.

Van Noort, M., Rommerts, F. F. G., Van Amerongen, A., & Wirtz, K. W. A. (1988a) *Biochem. Biophys. Res. Commun. 154*, 60–65.

Van Noort, M., Rommerts, F. F. G., Van Amerongen, A., & Wirtz, K. W. A. (1988b) *Mol. Cell. Endocrinol. 56*, 133–140.

Van Paridon, P. A., Visser, A. J. W. G., & Wirtz, K. W. A. (1987) *Biochim. Biophys. Acta 898*, 172–180.

Van Paridon, P. A., Gadella, T. W. J., Jr., Somerharju, P. J., & Wirtz, K. W. A. (1988) *Biochemistry 27*, 6208–6214.

Visser, A. J. W. G., Van Hoek, A., O'Kane, D. J., & Lee, J. (1989) *Eur. Biophys. J. 17*, 75–85.

Vos, K., Van Hoek, A., & Visser, A. J. W. G. (1987) *Eur. J. Biochem. 165*, 55–63.

Wasylewski, Z., Koloczek, H., & Wasniowska, A. (1988) *Eur. J. Biochem. 172*, 719–724.

Westerman, J., & Wirtz, K. W. A. (1985) *Biochem. Biophys. Res. Commun. 127*, 333–338.

Wirtz, K. W. A., & Gadella, T. W. J., Jr. (1990) *Experientia 46*, 592–599.

Wolber, P. K., & Hudson, B. S. (1981) *Biochemistry 20*, 2800–2810.

Zuker, M., Szabo, A. G., Bramall, L., Krajcarski, D. T., & Selinger, B. (1985) *Rev. Sci. Instrum. 56*, 14–22.